



UNIVERSITY OF LEEDS

This is a repository copy of *Preliminary Comparisons of Particulate Emissions Generated from Different Disc Brake Rotors*.

White Rose Research Online URL for this paper:

<https://eprints.whiterose.ac.uk/177272/>

Version: Presentation

Conference or Workshop Item:

Sanuddin, A, Gilkeson, C, Brooks, P et al. (3 more authors) (Accepted: 2021) Preliminary Comparisons of Particulate Emissions Generated from Different Disc Brake Rotors. In: Eurobrake 2021, 17 May - 21 Aug 2021, Online. (Unpublished)

This is an author produced version of a conference paper originally presented at Eurobrake 2021, 17-21 May 2021, held online.

Reuse

Items deposited in White Rose Research Online are protected by copyright, with all rights reserved unless indicated otherwise. They may be downloaded and/or printed for private study, or other acts as permitted by national copyright laws. The publisher or other rights holders may allow further reproduction and re-use of the full text version. This is indicated by the licence information on the White Rose Research Online record for the item.

Takedown

If you consider content in White Rose Research Online to be in breach of UK law, please notify us by emailing eprints@whiterose.ac.uk including the URL of the record and the reason for the withdrawal request.



eprints@whiterose.ac.uk
<https://eprints.whiterose.ac.uk/>

Preliminary Comparisons of Particulate Emissions Generated from Different Disc Brake Rotors

*Sanuddin, Asmawi^{1,2}, Kosarieh, Shahriar¹, Gilkeson, Carl¹, Brooks, Peter¹, Barton, David¹, Shrestha, Suman³

¹University of Leeds, United Kingdom

²Universiti Malaysia Perlis, Malaysia (E-mail: asmawi@unimap.edu.my)

³Keronite International Ltd., United Kingdom

DOI (FISITA USE ONLY)

ABSTRACT: Lightweight disc brake rotors have become a popular alternative to conventional grey cast iron (GCI). The thermal and tribological response of these brake rotors will differ during a braking operation. This may result in the generation of particulate wear debris with different characteristics, which can affect the environment and human health to different degrees. Studies have shown a relationship between adverse health effects and the characteristics of airborne particulate matter such as particle size, concentration and chemical composition. In this study, the particulate matter released from a novel lightweight disc brake rotor is compared to that released from the conventional grey cast iron rotor. The lightweight brake rotor was made of aluminium alloy (Al6082) and its rubbing surfaces were treated using the Plasma Electrolytic Oxidation (PEO) process. The process produced hard, dense, wear-resistant and well-adhered alumina coatings of approximate thickness 50 microns. A novel test rig was developed based upon the existing Leeds full-scale disc brake dynamometer. An enclosure was constructed around the brake assembly and ducting was carefully designed to ensure the cleanliness of the intake air to the system. Both brake rotors were tested under drag-braking conditions of constant sliding speed and applied braking pressure. Three braking test conditions with hydraulic pressures of 5, 10 and 15 bar at a constant speed of 135 rpm were selected from initial brake dynamometer tests. Braking test parameters of rotor rubbing surface temperature and coefficient of friction were measured during the tests and their effect on the brake wear particle characteristics were investigated. To measure and collect airborne brake wear particles, the Dekati ELPI+ unit was utilised along with a custom-made probe. This probe was made of stainless steel and its geometry was tailored to comply with the isokinetic concept. A scanning electron microscope (SEM) equipped with an energy-dispersive X-ray spectroscopy (EDX) system was utilised to investigate the morphology and chemical composition of the airborne brake wear particles collected by the Dekati unit. The initial comparison results showed that the PEO-treated lightweight aluminium alloy (PEO-Al) rotor has the potential not only to significantly reduce the unsprung mass of the vehicle but also reduce particulate matter emissions compared with the standard GCI rotor. The results also revealed that the percentage of iron contained in the PEO-Al debris was about threefold lower than that from the GCI rotor under all steady-state drag braking conditions studied which may have important health implications.

KEY WORDS: lightweight rotor, test rig, brake wear, Plasma Electrolytic Oxidation, brake dynamometer

1. INTRODUCTION

Stringent regulations on exhaust emissions have put automotive companies under tremendous pressure to improve vehicle fuel economy and subsequently reduce the emissions of CO₂. The use of lightweight disc brake rotors is one of the solutions to meet this legislative requirement. Recent studies have shown that aluminium alloy is a good alternative for replacing conventional ferrous materials because of its excellent properties such as low density, high specific heat and high thermal conductivity. Hussain (2018) indicates that for a medium-sized passenger car, the unsprung mass reduction can be estimated at around 20 kg by the use of aluminium alloy based material in the brake rotor. Despite its excellent properties, the lightweight aluminium brake rotor possesses some major limitations because of its thermomechanical properties. Such alloys have low maximum operating temperature and do not exhibit sufficient wear resistance. Therefore, it is essential to protect the rubbing surface of an aluminium rotor with high temperature

resistant materials such as alumina (Al₂O₃) or silicon carbide (SiC) (Agbeleye et al., 2020). The function of the substrate material can be improved by applying some form of surface treatment process. Plasma electrolytic oxidation (PEO) is one of the promising surface treatment used to modify the substrate surface into an excellent oxide layer properties. The PEO process is similar to the anodising process except much higher voltages are applied in the former (Gulden et al., 2020). The application of the PEO process produces coating layers of higher hardness, density and wear-resistance as well as better adhesion to the substrate compared to the anodising process. Alnaqi et al. (2014) reported that the PEO process improves the thermal and friction performance of the wrought aluminium brake rotor up to rubbing surface temperatures of 500°C.

Recently, a significant increase in airborne brake wear particulate matter (PM) in urban areas has attracted much interest among researchers from around the world. The brake wear particles are generated when sliding contact between the brake pads and the rotor takes place across the interface and the energy is dissipated

by the friction generated, which in turn drives the wear process. The brake wear particles are produced by the friction created when the brake pads squeeze against the rotor. They contribute significantly to non-exhaust emissions alongside tyre and road wear as well as resuspension of deposited road dust. Several studies reported that the non-exhaust emissions have become the major contributor to the traffic-related PM. Their proportion has surpassed the proportion of exhaust emissions every year and this trend is projected to increase even more in the future. The main reason behind this trend is the strict enforcement of regulations regarding exhaust emissions leading to a decline in use of diesel engines whereas no proper such regulations have been established for non-exhaust emissions (Perricone et al., 2016; Grigoratos and Martini, 2015; DEFRA, 2019).

Numerous studies have reported the relationship between adverse health effects and the characteristics of PM. It was shown that the particle size of PM is an important factor in influencing how the particles are deposited in the respiratory system and its subsequent effect on human health (Kumar et al., 2013; Pope et al., 2002). Samet et al. (2000) showed that the concentrations of PM in the environment may be associated with human mortality. There is consistent evidence linking the level of PM concentration with the mortality rate from cardiovascular and respiratory illnesses. Furthermore, the chemical composition of particles may also have similar effects on human health (Magari et al., 2002; Kelly and Fussel, 2012; Pope et al., 2007; Ostro et al., 2007). Toxic substances which typically include compounds of Fe, Cu, Ni, Cr, Zn, Al, Pb, Se, Pd and Mn are often discovered in PM. From the aforementioned effects, it is important to consider both size distributions and composition characteristics of brake wear debris.

Measurements of airborne brake-related PM in an open atmosphere is quite challenging because the airborne particles collected may originate from other sources. The changeable wind velocity and direction often affects the sampling results. Most of the research studies on brake wear particles found in the literature were conducted inside a laboratory either in open or closed systems. Since a standardised procedure is not available for this kind of experiment, a variety of test rigs and testing protocols have been constructed around the world. This has often led to different and even conflicting results. However, the basis of the findings is usually the same. Most of the studies attempted to observe the level of particle concentrations and the presence of chemical elements in brake wear debris. In this study, the performance of conventional GCI and PEO-Al rotors with regard to particle size and mass distribution, morphology and chemical composition was investigated and characterised for comparison purposes. The measurement of brake wear emissions was conducted using a newly developed test rig. The system was based upon the existing Leeds full-scale disc brake dynamometer which is designed to simulate real world drag brake applications.

2. EXPERIMENTAL SET-UP

2.1. Materials

Two kinds of brake rotor, namely the conventional GCI and PEO-Al rotors, were employed in the present study for investigating

airborne brake wear particle emissions. The commercial GCI rotor used was the Rover 75 brake rotor which has an outside diameter of 284 mm and an original thickness of 22 mm. This rotor was manufactured with a vented section inbetween the two braking contact surfaces to provide effective cooling for the part. The standard NAO brake pads (Mintex MDB1189) were utilised along with the Rover 75 rotor to form the friction pair. These commercial brake pads have a contact area of approximately 2400 mm² and they were fully bedded-in. The second brake rotor was designed and developed using in-house facilities. The rotor was constructed using lightweight aluminium alloy (Al-6082) as a substrate and the PEO treatment was applied to its rubbing surfaces by Keronite International Ltd. Generally speaking, the PEO-Al rotor consists of two separate parts containing the rubbing surfaces with a vented section inbetween. The completely assembled PEO-Al rotor has a thickness of 25 mm and an outside diameter of 280 mm. The brake pads used with this coated rotor were specially designed and supplied by TMD Friction. The contact area of each pad is approximately 2960 mm². The details regarding the formulation are confidential and remain the intellectual property of the company. Figure 1 shows images of the Rover 75 and PEO-Al brake rotors.

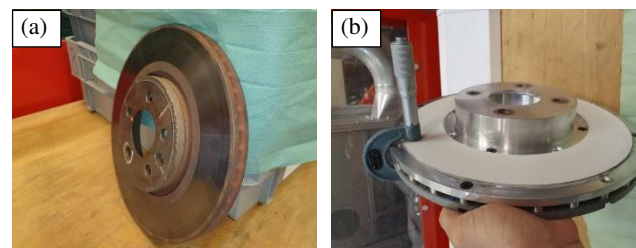


Figure 1: Physical appearance of (a) GCI and (b) PEO-Al brake rotors.

2.2. Test set-up

The determination of brake wear emissions is properly conducted inside a laboratory with control of the environment. Figure 2 shows photographs of the newly developed test rig for generating, measuring and collecting the brake wear particle emissions. A custom-made hexahedral Perspex box was constructed at the brake end of the main dynamometer shaft in order to seal the air in the immediate vicinity of the brake assembly and keeping it separate from the laboratory air. The enclosure is connected to HEPA (H14) filters through ducting systems. An inlet duct connects the laboratory air via an inlet HEPA filter to the enclosure while an outlet duct connects the enclosure to an outlet HEPA filter. A further piece of ductwork connects the outlet HEPA filter to a fan with a 4 kW rating on the top of the building. All the ducts were made of galvanised sheet steel and have an inside diameter of 225 mm.

Airflow within the enclosure is controlled by the fan to deliver fresh air through the inlet duct, before it mixes within the brake enclosure and exits through an outlet duct. Incoming and outgoing air is cleaned using the HEPA filters and vented safely to atmosphere on the top of the building. As a safety precaution, a carbon activated filter was employed at the outlet to remove any strong odour and other harmful gases. The speed of the fan can be adjusted by controlling the fan setting to create an air velocity in the range of 6

to 15 m/s. The measurement of the air velocity was carried out using an anemometer at the velocity test point.

Within the outlet duct, four tappings (T1 – T4) and a velocity test point (VTP) were provided for sampling brake wear particulate matter and measuring airflow velocity, respectively (see Figure 2). A custom-made sampling probe was utilised at the tap locations to extract representative samples for analysis. The probe geometry and air sampling volume flow rate are tailored using isokinetic sampling concept to avoid biased results and errors. To measure and capture brake wear debris, the Dekati ELPI®+ Electrical Low Pressure Impactor is connected to the isokinetic probe at its inlet and a vacuum pump at its outlet using a rubber hose and a vacuum hose, respectively. The ELPI®+ unit allows measurement of airborne particle size distribution and concentration in real time with a sampling rate of 1 Hz or 10 Hz. The instrument measures particles in 14 size stages from 6 nm to 10 μm . The 14 impactor stages (including a back-up filter stage) make it possible to collect airborne particles on filters for gravimetric and chemical analyses. This unit operates correctly at the sample flow rate of 10 litres/minute and this flow rate can be obtained by adjusting the impactor low pressure to 40 mbar (± 5 mbar).

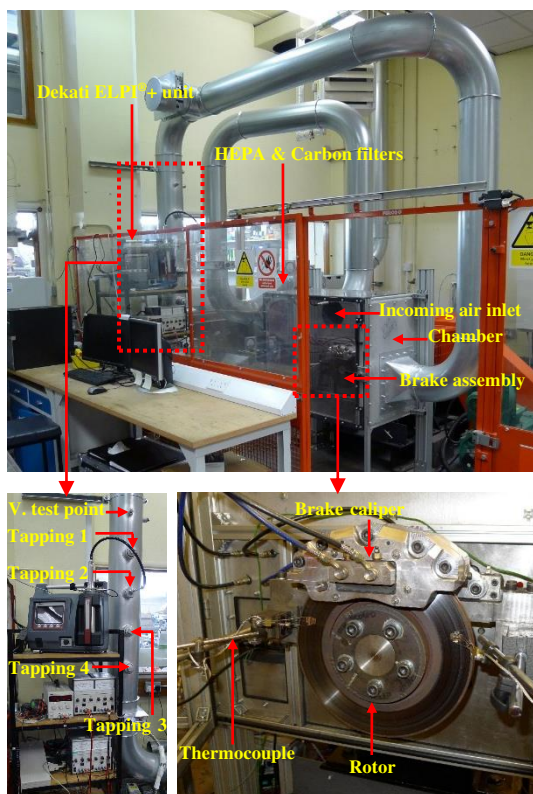


Figure 2: Photographs of the newly developed test rig.

2.3. Experimental procedures

Preliminary dynamometer tests were conducted for the GCI rotor to discover appropriate parameters for use in subsequent brake wear emission measurements. These parameters, namely hydraulic pressure and rotor rotational speed, were selected based on the temperature generated at the rubbing surface of the rotor during a drag braking event. It was anticipated that the temperature would

attain a steady-state condition following a few minutes after a test commenced. Three conditions that achieved nearly constant temperatures of 200, 300, and 400°C were selected. Iijima et al. (2007) have mentioned that the rotor temperature of 200°C is more representative of braking during urban driving, while the other two temperatures are produced under extreme braking, such as during a steep hill descent.

Hydraulic pressures of 5, 10 and 15 bar at a constant speed of 135 rpm were selected as the three braking conditions for subsequent tests and the corresponding steady-state temperatures achieved are 190, 315 and 410°C. These conditions closely achieve the desired rotor surface temperatures of 200, 300 and 400°C. The same brake conditions were used for the PEO-Al rotor tests to allow valid comparisons with those of the GCI rotor. At the time of this writing however, the test under the 15 bar pressure condition used for the GCI rotor could not be conducted for the PEO-Al rotor due to the COVID-19 lock-down restrictions.

A standard test procedure was established to generate, measure and collect airborne brake wear particles for both GCI and PEO-Al rotors. Real-time particle measurements and collections of the particles followed the same established procedure. For particle collections, no system background was recorded (the rotor is in stationary condition). Under drag brake conditions, the temperature of the rotor rubbing surface was recorded as hydraulic pressures were varied. The fan power was set at 5% of the total capacity in order to generate a velocity of ~ 7 m/s at the velocity test point. The duration of each braking test was 90 minutes to ensure that the rotor surface temperature reached a steady state. Prior to the tests, the background level of the system was measured for 10 minutes. For real-time particle measurements, the tests were conducted 3 times to obtain a repeatable result. Aluminium and polycarbonate (PC) foils were used for the particle measurements and collections, respectively. In the case of particle collections, only five PC foils were used in order to collect particles in the range of 1 μm – 10 μm (stages 10-14) because this larger scale range was of most interest due to its high mass fraction. In addition, the brake wear particles that fell down on the bottom of the enclosure were also collected on a PC foil. The position of the foil placed on the bottom of the enclosure (underneath the trailing end of the caliper) is shown in Figure 3.

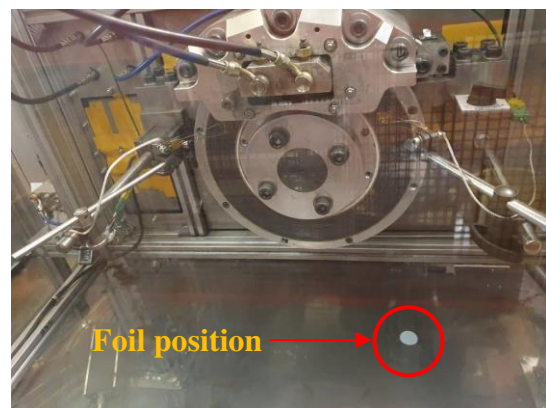


Figure 3: PC foil position on the bottom of the enclosure for PEO-Al rotor test.

2.2. Characterisation tests

Particle samples collected from the tests of both GCI and PEO-Al rotors were characterised using the Hitachi TM3030Plus SEM. Particle sizes and distributions were examined using scanning electron microscope (SEM) while chemical compositions of the collected particles were analysed using energy-dispersive X-ray spectroscopy (EDX) techniques.

3. RESULTS AND DISCUSSION

3.1. Brake wear particle measurements

3.1.1. Thermal performance

Tests were repeated three times at each braking condition applied for both brake rotors in order to check for repeatability. All tests follow the same sampling procedure as described previously. The rotor surface temperature was measured near the leading edge of the brake rotor using a K-type rubbing thermocouple as shown in Figure 2. Figure 4 shows the temperature-time history plot for all tests. Annotations in the figure legend have the following meaning; 'P' represents hydraulic pressure, 'A', 'B' and 'C' represent the 3 repetitions for GCI rotor and 'D', 'E' and 'F' represent the 3 repetitions for PEO-Al rotor.

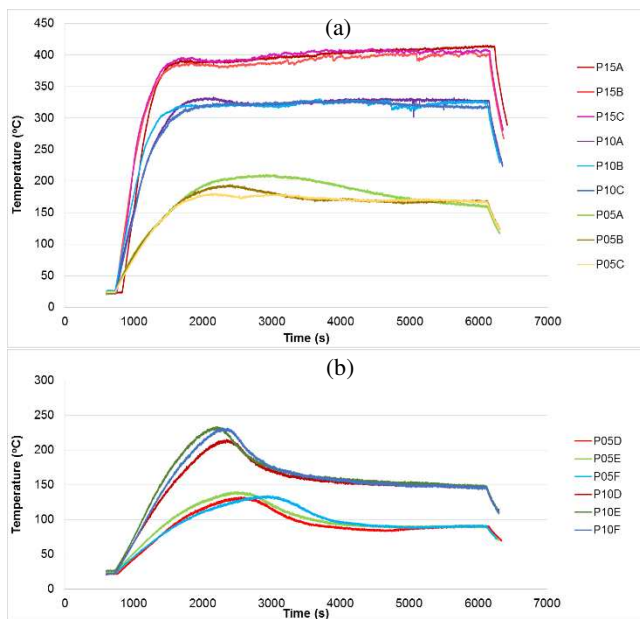


Figure 4: Rotor temperature variation with time for the three tests at each braking condition of (a) GCI and (b) PEO-Al rotors.

For the GCI rotor (see Figure 4 (a)), the results show all temperatures attain a steady-state condition following a few minutes of the braking process except for the test of P05A where the temperature gradually decreases after reaching a maximum value. The test results at 5, 10 and 15 bar show nearly constant steady-state temperatures of approximately 170, 320 and 400°C, respectively. Overall, these results confirm that good consistency has been achieved for the three braking conditions, although the result of P05A demonstrates a slight difference from the other results at this low pressure. In the case of PEO-Al, the results show that all rotor temperatures attain a steady-state condition after about 3000 seconds from commencement of the braking event. The test results at 5 bar and 10 bar demonstrate nearly constant steady-state temperatures of 90°C and 150°C, respectively. Generally, the results in Figure 4 (b) suggest that the two brake conditions have

achieved good consistency. It can also be seen from Figure 4 that the temperatures of the GCI rotor are higher than those of the PEO-Al rotor for the same brake pressure applied. This is at least partly due to the higher frictional torque generated by the GCI system leading to a higher thermal power input to the GCI rotor and hence higher temperatures.

3.1.2. Friction performance

Figure 5 shows the variation of the measured coefficient of friction (COF) with time for both GCI and PEO-Al rotors at 5 and 10 bar brake pressures. These results are typical of braking events during the real-time particle measurements. From this figure, it can be seen that the COF does not significantly change as the brake pressure for the two brake rotor materials is increased. Initially, the coefficient of friction rises rapidly for both GCI and PEO-Al rotors, and then reaches a peak at about 0.6 for both rotors before dropping to a nearly constant steady-state value in the range 0.43-0.49 for the GCI rotor and in the range 0.25-0.28 for the PEO-Al rotor. The steady-state condition obtained suggests that there is no sign of thermal fade occurring for the GCI rotor during this time period. In contrast, the COF of the PEO-Al rotor attains a maximum value after about 2000 seconds and then decreases before reaching a nearly steady-state condition. The reduction of COF may be correlated with thermal fade phenomena that may occur when the brake torque is maintained over a long period of time at high rotor temperature.

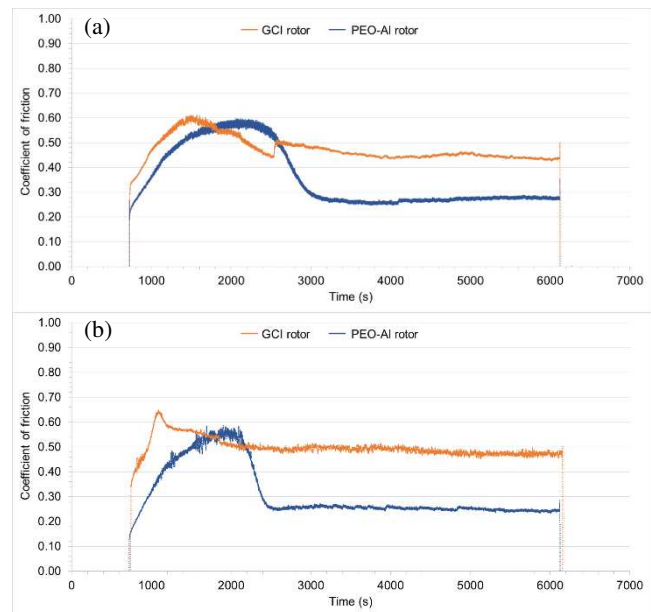


Figure 5: Temporal changes in the coefficient of friction for the two brake rotor materials at (a) 5 and (b) 10 bar brake pressures.

The present results confirm that the GCI rotor has a significantly higher long term steady-state COF than the PEO-Al rotor. This could be due to the different compositions in the friction material used for the tests on the two rotors which may affect the steady-state COF. The apparent difference is that a high percentage of Ba was found only in the friction material of the GCI rotor while a high percentage of Cu was found only in the friction material of the PEO-Al rotor (see Section 3.2.2). The higher and more stable value of COF for the GCI rotor indicates that this rotor-pad system has resulted from a long programme of development to produce the current state-of-the-art friction pair employed by most road vehicles. The lower and more variable COF of the PEO-Al rotor may reflect the much shorter time of development of the friction material for this rotor as compared to that for GCI. It is also worth

pointing out that the vast majority of brake applications on the road are of much shorter duration than the long drag applications studied here. The fact that the PEO-Al rotor reaches a relatively high COF of about 0.6 only slightly more slowly after brake application than the GCI rotor is a promising sign that this lightweight rotor may be suitable for on-road use.

3.1.3. Particle mass distribution

Figure 6 shows the comparison of particle mass concentration for both brake rotor materials studied at 5 and 10 bar brake pressures. The figure also shows the mass concentrations of the test at 15 bar for the GCI rotor. The mass distributions highlight a noticeable difference between background and brake application measurements, particularly for the coarse particle fractions. This confirms that significant numbers of airborne particles generated from the PEO-Al disc brake friction pair were captured during the braking event. In the case of GCI rotor, the mass fraction of coarser particles marginally increases when the brake pressure decreases from 15 to 10 bar, at a constant speed of 135 rpm. However, a much more significant increase occurs in the 1-10 μm range when the pressure is reduced to 5 bar. This may be due to more wear debris becoming trapped between the brake pads and rotor at higher brake pressures. More precise reasons behind this inverse relationship could not be inferred with the current available data. However, this finding was validated by the gravimetric analysis which showed similar results. For the PEO-Al rotor, the mass fraction of coarser particles somewhat increases as the brake pressure increases.

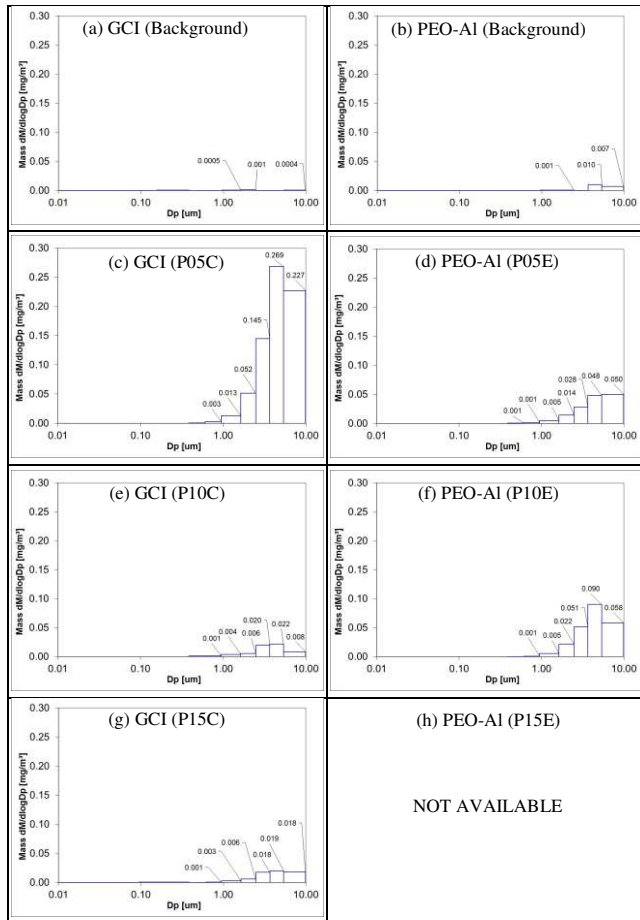


Figure 6: Particle mass distribution measurements for (a, c, e & g) GCI and (b, d, f & h) PEO-Al rotors at the corresponding 5, 10 & 15 bar hydraulic pressures.

Figure 6 clearly shows that the particle mass concentration of all the coarser particle fractions at 5 bar brake pressure is significantly greater for the GCI rotor as compared to the PEO-Al rotor. However, for the brake pressure of 10 bar, the particle mass concentration of the PEO-Al rotor for particle size fractions greater than 1 μm is somewhat greater than that of the GCI rotor. It is estimated that greater than 90% of the total brake particulate mass is emitted as particles in this 1 to 10 μm (PM_{1.0} - PM₁₀) size range for both brake rotor materials.

3.1.4. Overall average particulate mass distributions

Figure 7 shows the particle mass concentrations in the PM_{0.1}, PM_{2.5} and PM₁₀ size ranges averaged over all three repeated tests at both pressures for the two brake rotor materials studied. The figure also shows the average concentrations of the test at 15 bar for the GCI rotor. From Figure 7 (a), the particle mass concentrations in the PM_{2.5} and PM₁₀ are higher at the lower brake pressure and temperature for the GCI rotor. From Figure 7.6 (b), however, the concentrations in these two larger PM size ranges are higher at the higher brake pressure and temperature for the PEO-Al rotor. At 5 bar brake pressure, the PM₁₀ category contributes 90% and 83% of the total airborne brake wear emissions by mass for the GCI and PEO-Al rotors, respectively. At 10 bar brake pressure, the corresponding proportions are 81% and 87% of the total mass, respectively. These results show that GCI emissions of coarser particle fractions (2.5 to 10 μm) are slightly higher than PEO-Al emissions at 5 bar brake pressure whereas the latter are slightly higher at 10 bar brake pressure. For the brake pressure of 5 bar, the particle mass concentration for the PEO-Al rotor in the PM_{2.5} and PM₁₀ categories is reduced by factors of 2.9 and 5.4, respectively, compared with the GCI rotor. On the other hand, for the brake pressure of 10 bar, the particle mass concentration of PEO-Al rotor in the PM_{2.5} and PM₁₀ categories is increased by factors of 1.7 and 2.6, respectively. These findings indicate that PM_{2.5} and PM₁₀ emissions of the PEO-Al rotor are much lower than those of GCI rotor at 5 bar brake pressure whilst, for the higher brake pressure, these two PM categories are marginally higher for the PEO-Al rotor.

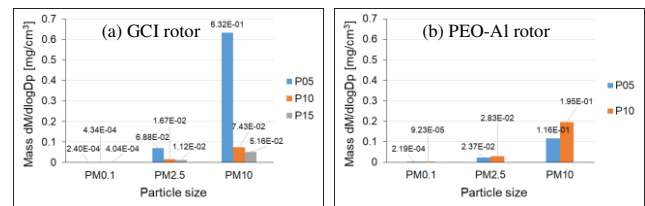


Figure Error! No text of specified style in document.: Brake wear emissions of PM_{0.1}, PM_{2.5} and PM₁₀ based on average particle mass concentrations for the two brake rotor materials.

3.2. Post-test PM characterisation

3.2.1. Microstructural analysis

SEM observations were conducted on the brake wear debris collected on the foils at a magnification level of 6000x for both brake rotor materials. All micrographs taken from the different stages of ELPI[®] are exhibited in Figures 8 and 9 for brake pressures of 5 and 10 bar, respectively. The images taken from the PC foils positioned on the bottom of the enclosure at 3000x magnifications are exhibited in Figure 10 for the two braking

conditions and brake rotor materials studied. However, the results for GCI rotor at 15 bar hydraulic pressure are not presented in this paper. The amount of wear debris collected in this test was fewer than those of the other two lower brake pressure test conditions for all stages of ELPI[®]+ studied.

In terms of particle size, most of the particles are classified and registered correctly in the corresponding stages for both braking conditions and brake rotor materials studied. Nevertheless, some finer particles could be seen on a stage with a larger size interval. This phenomenon might be due to the effects of diffusion as the fine particles passed through the preceding stage. At the same time, there is also a small number of coarse particles deposited on finer stages. This might be caused by the particle bounce and blow-off effects that could happen to larger particles which fall from the stages they should be captured on to lower stages

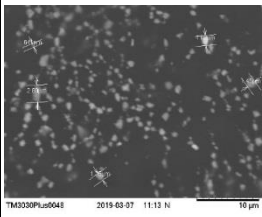
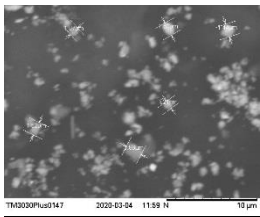
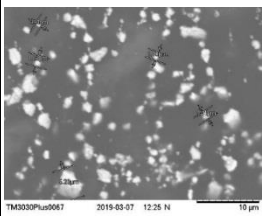
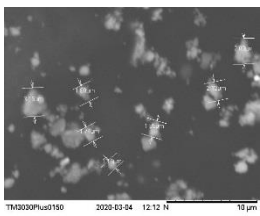
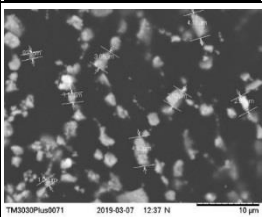
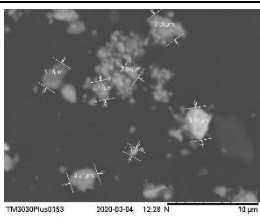
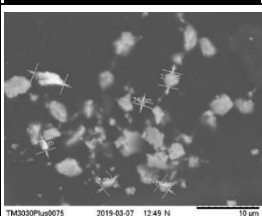
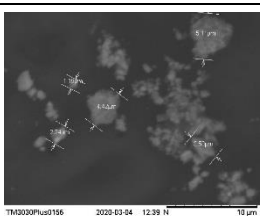
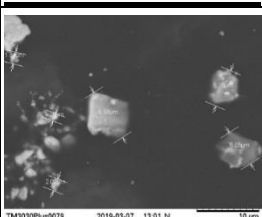
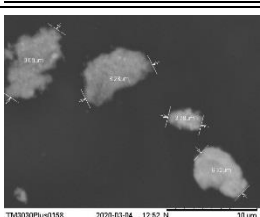
Stage & Size (µm)	Particle images (6000x)	
	GCI	PEO-Al
(a) Stage 10 (0.949 – 1.63)		
(b) Stage 11 (1.630 – 2.47)		
(c) Stage 12 (2.470 – 3.66)		
(d) Stage 13 (3.660 – 5.37)		
(e) Stage 14 (5.370 – 9.90)		

Figure 8: Micrographs of the 5 bar hydraulic pressure test for the two brake rotor materials.

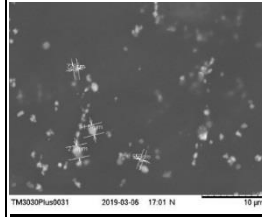
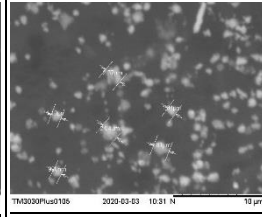
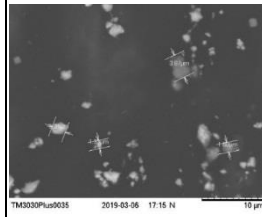
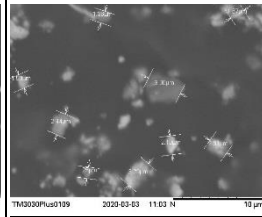
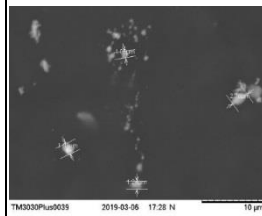
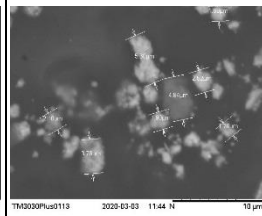
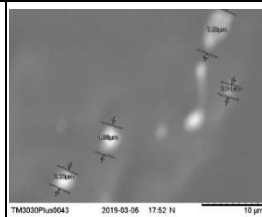
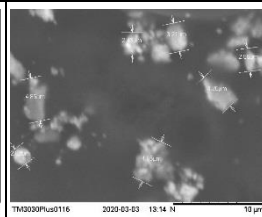

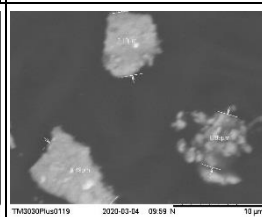
Stage & Size (µm)	Particle images (6000x)	
	GCI	PEO-Al
(a) Stage 10 (0.949 – 1.63)		
(b) Stage 11 (1.630 – 2.47)		
(c) Stage 12 (2.470 – 3.66)		
(d) Stage 13 (3.660 – 5.37)		
(e) Stage 14 (5.370 – 9.90)		

Figure 9: Micrographs of the 10 bar hydraulic pressure test for the two brake rotor materials.

For the test at 5 bar brake pressure, it can be seen from Figure 8 that the distribution of brake wear debris for both GCI and PEO-Al rotors demonstrates a similarity whereby the number of observable particles for both results reduces from fine to coarse particles. However, greater numbers of brake wear debris can be noticed for the GCI rotor when comparing the same ELPI+ stage results. Micrographs obtained from both brake rotor materials do not reveal any significant differences in the particle shape for the different stages, most particles being irregular in shape. The micrographs for these two rotor materials also do not show the presence of wear particle agglomerates. However, the tendency of collected particles to form clusters of wear debris can be seen in the finer particle stages. For the test at 10 bar brake pressure (see Figure 9), the results also show no difference in particle shape and agglomerated formation. However, particles are noticeably more concentrated in the results for the PEO-Al rotor. These micrographs indicate that

the higher the brake pressure the more abundant the particles collected in the case of PEO-Al rotor but the opposite is apparent for the GCI rotor where more particles are observed at the lower brake pressure. This qualitative result is consistent with the quantitative measures of particle mass distribution which were obtained from the real-time particle measurement.

For the particles collected on the foils at the bottom of the enclosure (see Figure 10), both micrographs show the presence of particles with varying sizes, most of which are less than 10 μm in size. There are no significant differences between the results of GCI and PEO-Al rotors for the two brake conditions applied (5 and 10 bar). Particle agglomeration and numerous particles with an irregular shape were observed in all these enclosure debris results.

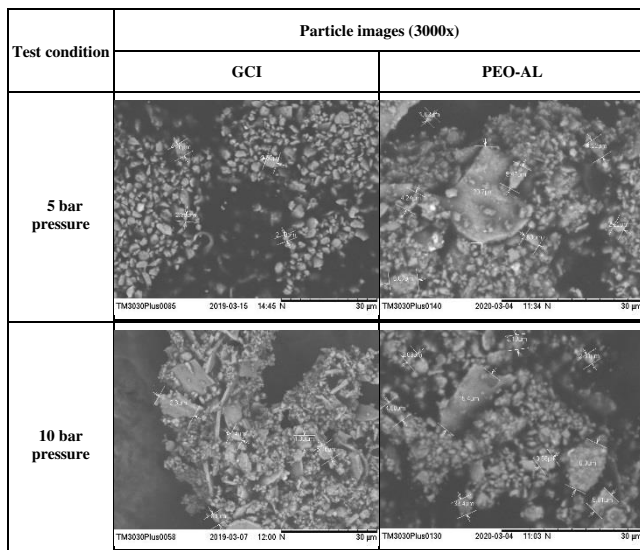


Figure 10: Micrographs of the collected particles on the bottom of the enclosure for both braking conditions and brake rotor materials studied.

3.2.2. Elemental composition evaluation

The EDX analysis showed that there are seven main elements (Fe, Ba, Cr, Ca, S, Si, Al) and eight key elements (Fe, Cu, Cr, Ca, S, Si, Al and Mg) were found in the GCI and PEO-Al brake wear debris, respectively. For the purpose of comparisons, only Fe, Al and S were considered. Figure 11 shows the weight percentage comparison of these three key elements for both brake rotor materials. The EDX quantitative analysis was determined without considering oxygen and carbon due to the overabundance of these elements in the PC foils that most likely originate from the PC foil. Moreover, this quantitative analysis is not reliable for light elements (Verma et al., 2016).

Overall, it can be estimated from Figure 11 that the percentage of Fe in the PEO-Al debris is about threefold lower than that from the GCI rotor. The distributions of the Fe percentage are somewhat uniform across all the size ranges for both brake conditions and rotor materials studied. A similar pattern of the results was obtained in a previous study (Verma et al., 2016). In the case of the GCI rotor, Iijima et al. (2007) and Hagino et al., (2016) also found that Fe was a major element of wear debris and that large amounts of Fe were assumed to come from the brake rotor. At a much smaller proportion, the percentage of Al in the PEO-Al debris is about four

times greater than that for the GCI rotor. The distribution of the Al percentage is quite uniform for the PEO-Al rotor but this is not the case for the GCI rotor where it appears quite random. The percentage of S in the PEO-Al debris is nearly half that from the GCI rotor and the distribution of the S is more uniform in the PEO-Al rotor.

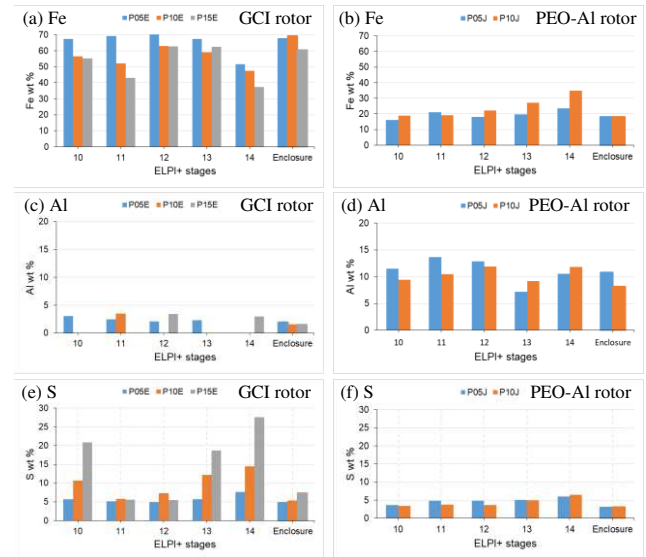


Figure 11: Comparison of elemental percentages by weight for two brake rotor materials at 5 and 10 bar brake pressures (a & b) Fe, (c & d) Al and (e & f) S.

The EDX analysis also revealed high percentages of Ba and Cu found only in the GCI and PEO-Al brake rotors, respectively. It might also be worth comparing the weight percentages of these two elements which are assumed to originate from the respective brake pad materials. The presence of Ba might be derived from the barium sulphate, BaSO_4 compound which is employed as a filler in brake pads in order to improve noise and also reduce manufacturing cost. Cu usually has the highest weight percentage (excluding C and O) at all size fractions. Most brake pad manufacturers have recently reduced and even eliminated copper in their products. The copper has usually been used to help heat dissipation in the pad, but the problem is that it produces dust that can be toxic to aquatic life. However, the pad material used in these tests was a special formulation designed to produce stable friction against the PEO coating and this may have contained more Cu than is now common. Figure 12 shows a comparison of elemental weight percentages of Ba (from GCI rotor) and of Cu (from PEO-Al rotor) for the two brake pressures studied. The percentage of Cu in the PEO-Al rotor is shown to be about twice that of Ba in the GCI rotor across all size ranges.

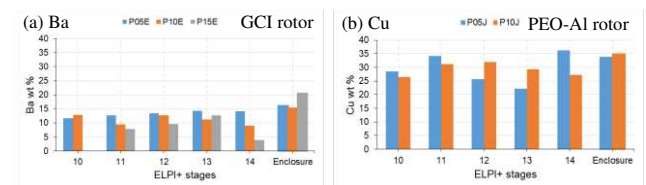


Figure 12: Comparison of weight percentages for two different elements, (a) Ba and (b) Al at 5 and 10 bar brake pressures.

4. CONCLUSION

This work presents the generation, measurement and collection of airborne brake wear particles under controlled drag brake conditions of constant sliding speed and applied braking pressure using the modified brake dynamometer. The performance of the novel PEO-treated lightweight disc brake rotor has been investigated and compared with a grey cast iron rotor (GCI), particularly with respect to the emission of the brake wear particles in the environment. Overall, it was concluded that the PEO-treated lightweight aluminium alloy rotor (PEO-Al) showed a better performance than the conventional GCI rotor in terms of both mass reduction and fewer wear debris particle emissions, especially at low applied pressures. However, the PEO-Al rotor showed less consistent and generally lower friction coefficients than the GCI, indicating the need to further develop and optimise the pad material for rubbing against the PEO-Al disc. Other significant findings of this study are summarized as follows:

- 1) The particle number and mass concentrations in the coarser particle fractions (1.0-10 µm) collected by the Dekati impactor showed a decreasing trend as the brake pressure was increased for the GCI rotor. However, this relationship was opposite for the PEO-Al rotor for the two braking conditions studied i.e. the emissions were increased at 10 bar compared with 5 bar brake pressure.
- 2) The results revealed that the PM₁₀ (PM_{2.5}-PM₁₀) category contributed about 85% of the total airborne brake particulate mass emissions for the PEO-Al rotor at both brake pressures studied, while the PM₁₀ also accounted for greater than 80% of the total mass for the GCI rotor at 5, 10 and 15 bar brake pressures.
- 3) The particle mass concentrations of the PEO-Al rotor in the PM_{2.5} and PM₁₀ categories for the brake pressure of 5 bar were reduced by factors of 2.9 and 5.4, respectively, compared with the GCI rotor. At the higher pressure of 10 bar, these concentrations were increased by factors of 1.7 and 2.6, respectively.
- 4) Based on the EDX analysis, the Fe content in the PEO-Al debris was found to be about threefold lower than that from the GCI rotor. The percentage of Fe increased with the increased brake pressure for the PEO-Al rotor whereas this relationship was opposite for the GCI rotor results. However, the content of Al in the former was about four times greater than that for the GCI. This is as expected given the main constituent elements of the two brake rotors.

REFERENCES

- Agbeleye, A.A., Esezobor, D.E., Balogun, S.A., Agunsoye, J.O., Solis, J. and Neville A. 2020. Tribological properties of aluminium-clay composites for brake disc rotor applications. *Journal of King Saud University – Science*. 32(1), pp.21-28.
- Alnaqi, A.A. 2014. *Characterisation of coated lightweight brake rotors*. Doctor of Philosophy thesis, University of Leeds.
- DEFRA. 2019. *Non-exhaust emissions from road traffic*. United Kingdom: Department for Environment, Food and Rural Affairs.
- Grigoratos, T. and Martini, G. 2015. Brake wear particle emissions: a review. *Environmental Science and Pollution Research*. 22, pp.2491-2504.
- Gulden, F., Reinhold, B., Gramstat, S., Stich, A., Tetzlaff, U. and Höppel, H.W. 2020. Investigation of the run-in and corrosion behavior of a PEO-coated aluminum brake disc. In: Pfeffer, P. ed. *10th International Munich Chassis Symposium 2019*. Proceedings, Wiesbaden: Springer Vieweg, pp.611-631.
- Hagino, H., Oyama, M. and Sasaki, S. 2016. Laboratory testing of airborne brake wear particle emissions using a dynamometer system under urban city driving cycles. *Atmospheric Environment*. 131, pp.269-278.
- Hussain, J. 2018. *Thermal and material characterisation of coated lightweight disc brake rotor*. Doctor of Philosophy thesis, University of Leeds.
- Iijima, A., Sato, K., Yano, K., Tago, H., Kato, M., Kimura, H. and Furuta, N. 2007. Particle size and composition distribution analysis of automotive brake abrasion dusts for the evaluation of antimony sources of airborne particulate matter. *Atmospheric Environment*. 41(23), pp.4908-4919.
- Kelly, F.J. and Fussell J.C. 2012. Size, source and chemical composition as determinants of toxicity attributable to ambient particulate matter. *Atmospheric Environment*. 60, pp.504-526.
- Kumar, P., Pirjola, L., Ketzel, M., and Harrison, R.M. 2013. Nanoparticle emissions from 11 non-vehicle exhaust sources - a review. *Atmospheric Environment*, 67, pp.252-277.
- Magari, S.R., Schwartz, J., Williams, P.L., Hauser, R., Smith, T.J. and Christiani, D.C. 2002. The association of particulate air metal concentrations with heart rate variability. *Environmental health perspectives*. 110(9), pp.875-880.
- Ostro, B., Feng, W.Y., Broadwin, R., Green, S. and Lipsett, M. 2007. The effects of components of fine particulate air pollution on mortality in California: results from CALFINE. *Environmental Health Perspectives*. 115(1), pp.13-19.
- Perricone, G., Wahlström, J. and Olofsson, U. 2016. Towards a test stand for standardized measurements of the brake emissions. *Proceedings of the Institution of Mechanical Engineers, Part D: Journal of Automobile Engineering*. 230(11), pp.1521-1528.
- Pope III, C.A., Burnett, R.T., Thun, M.J., Calle, E.E., Krewski, D., Ito, K. and Thurston, G.D. 2002. Lung cancer, cardiopulmonary mortality, and long-term exposure to fine particulate air pollution. *The Journal of the American Medical Association*. 287(9), pp.1132-1141.
- Pope III, C.A., Rodermund, D.L. and Gee, M.M. 2007. Mortality effects of a copper smelter strike and reduced ambient sulfate particulate matter air pollution. *Environmental Health Perspectives*. 115(5), pp.679-683.
- Samet, J.M., Dominici, F., Currier, F.C., Coursac, I. and Zeger, S.L. 2000. Fine particulate air pollution and mortality in 20 U.S. cities, 1987-1994. *New England Journal of Medicine*. 343, pp.1742-1749.
- Verma, P.C., Alemani, M., Gialanella, S., Lutterotti, L., Olofsson, U. and Straffelini, G. 2016. Wear debris from brake system materials: a multi-analytical characterization approach. *Tribology International*. 94, pp.249-259.

ACKNOWLEDGEMENTS

TMD Friction for the supply of the pad material for the PEO rotor. The lead author would also like to thank the Malaysian government for the Scholarship provided to enable him to undertake this work at Leeds.